Origin of the avian predentary and evidence of a unique form of cranial kinesis in Cretaceous ornithuromorphs

Alida M. Bailleul[a,b,1], Zhiheng Li[a,b], Jingmai O'Connor[a,b], and Zhonghe Zhou[a,b,1]

[a]Key Laboratory of Vertebrate Evolution and Human Origins, Institute of Vertebrate Paleontology and Paleoanthropology, Chinese Academy of Sciences, 100044 Beijing, China; and [b]Center for Excellence in Life and Paleoenvironment, Chinese Academy of Sciences, 100044 Beijing, China

Contributed by Zhonghe Zhou, October 14, 2019 (sent for review July 11, 2019; reviewed by Anthony Herrel and Adam K. Huttenlocker)

The avian predentary is a small skeletal structure located rostral to the paired dentaries found only in Mesozoic ornithuromorphs. The evolution and function of this enigmatic element is unknown. Skeletal tissues forming the predentary and the lower jaws in the basal ornithuromorph *Yanornis martini* are identified using computed-tomography, scanning electron microscopy, and histology. On the basis of these data, we propose hypotheses for the development, structure, and function of this element. The predentary is composed of trabecular bone. The convex caudal surface articulates with rostromedial concavities on the dentaries. These articular surfaces are covered by cartilage, which on the dentaries is divided into 3 discrete patches: 1 rostral articular cartilage and 2 symphyseal cartilages. The mechanobiology of avian cartilage suggests both compression and kinesis were present at the predentary–dentary joint, therefore suggesting a yet unknown form of avian cranial kinesis. Ontogenetic processes of skeletal formation occurring within extant taxa do not suggest the predentary originates within the dentaries, nor Meckel's cartilage. We hypothesize that the predentary is a biomechanically induced sesamoid that arose within the soft connective tissues located rostral to the dentaries. The mandibular canal hosting the alveolar nerve suggests that the dentary teeth and predentary of *Yanornis* were proprioceptive. This whole system may have increased foraging efficiency. The Mesozoic avian predentary apparently coevolved with an edentulous portion of the premaxilla, representing a unique kinetic morphotype that combined teeth with a small functional beak and persisted successfully for ∼60 million years.

predentary | birds | sesamoid | kinesis | proprioception

The predentary (PD) is a bone located just rostral to the paired, unfused dentaries (DEs). This element is rare, only found in 3 groups of extinct vertebrates: Actinopterygian fishes (1–3), ornithischian dinosaurs (4), and Cretaceous nonneornithine ornithuromorph birds (5–8). Among extant taxa, a structure referred to as the PD is known in some (but not all) sailfishes and marlins of the Istiophorid family (actinopterygians) (3, 9), although the development of the PD in this lineage has yet to be investigated. The disparate distribution of this element among vertebrates does not favor any hypothesis of homology and parsimony strongly suggests that the PD in actinopterygians, ornithischians, and Cretaceous nonneornithine ornithuromorph birds all evolved independently, resulting in the proposal that the avian PD be alternatively referred to as the intersymphyseal ossification to avoid mistaken inferences regarding homology with the ornithischian PD (*SI Appendix*, Fig. S1) (10). However, because the ossification is not strictly intersymphyseal, in fact located rostral to the DEs and the mandibular symphysis, we will refer to the PD in nonneornithine ornithuromorphs as the "avian PD" (APD).

The APD was first described in the Late Cretaceous ornithurines *Hesperornis* and *Parahesperornis* (8). Although no PD has ever been recovered in the ornithurine *Ichthyornis* (11), the morphology of its dentaries strongly suggests a PD was also present in this species (7, 8). More recently, it has been identified in 5 species of nonornithurine ornithuromorphs from the Early Cretaceous Jehol Biota of northeastern China (*SI Appendix*, Fig. S2) (5, 7). Because all extant birds lack this bone, it was hypothesized that the APD was a common feature of Cretaceous ornithuromorphs that was subsequently lost (6). Additionally, the APD is apparently only present in toothed birds, being absent in all known specimens of the edentulous *Archaeorhynchus* (12–14).

This study aims to shed light on the origin and the function of the APD. No developmental hypothesis for the APD has ever been proposed. Based on its anatomical location, we see 3 possibilities: It may be that it originated within Meckel's cartilage, which belongs to the splanchnocranium (developmental hypothesis 1), or it may have arisen from the DEs (developmental hypothesis 2), in which case the APD would be of dermatocranial origin (15–17). A third possibility is that the APD is a sesamoid (e.g., ref, 18) that arose ectocranially within the connective tissues located rostral to the DEs (developmental hypothesis 3). Meckel's cartilage first arises within the developing skull as a primary cartilage model, which then gets partially replaced by bone through the process of endochondral ossification, whereas the DEs are membrane (dermal) bones that arise directly from

Significance

The avian predentary is a small, rarely preserved skeletal structure found only in toothed Mesozoic ornithuromorph birds. The origin and function of this enigmatic bone is poorly understood. Based on skeletal tissue identification in a specimen of the Early Cretaceous *Yanornis martini*, we propose developmental, structural, and functional hypotheses for this element. It consists of trabecular bone with a caudal articular surface for the dentary covered by cartilage. Tissue mechanobiology suggests this contact was kinetic, representing a previously unknown type of avian cranial kinesis. We hypothesize that the avian predentary was a biomechanically induced sesamoid that coevolved with an edentulous portion of the premaxilla, together representing a successful morphotype that combined a small beak with a proprioceptive system.

Author contributions: A.M.B., Z.L., J.O., and Z.Z. designed research; A.M.B., Z.L., J.O., and Z.Z. performed research; Z.Z. contributed new reagents/analytic tools; A.M.B. and Z.L. collected the data; A.M.B., Z.L., J.O., and Z.Z. analyzed data; and A.M.B. and J.O. wrote the paper.

Reviewers: A.H., Muséum National d'Histoire Naturelle; and A.K.H., University of Southern California.

The authors declare no competing interest.

Data deposition: We have deposited large computed tomography data in the Open Science Framework, OSF, https://osf.io/q9xsp/.

[1]To whom correspondence may be addressed. Email: alida.bailleul@ivpp.ac.cn or zhouzhonghe@ivpp.ac.cn.

This article contains supporting information online at https://www.pnas.org/lookup/suppl/doi:10.1073/pnas.1911820116/-/DCSupplemental.

First published November 18, 2019.

the cephalic mesenchyme via ossification centers without going through a primary cartilage model (15, 17). The distribution and identification of skeletal tissues, such as bone and cartilage, are key to differentiating between these competing hypotheses, as these tissues reflect different embryological origins within the skull.

The function of the APD is also mysterious. It has been noted that it is always associated with an edentulous rostral portion of the premaxillae (PM) dorsally overlapping the PD (7). This may suggest that these features coevolved, possibly representing an early stage in the evolution of the beak in the Ornithuromorpha, a clade in which a beak evolved multiple times [including that of the Neornithes but also in the *Archaeorhynchus* and *Eogranivora* lineages and others (14, 19)]. The DE–PD junction has been interpreted as a synovial joint linked to a piscivorous diet (7), but details beyond gross morphology are necessary to truly understand the function of this skeletal feature and the tissues linking it to the rest of the lower jaws. In addition to providing clues reflecting different embryological origins (e.g., dermatocranial, splanchnocranial, or ectocranial), bone and cartilage are also a direct reflection of the biomechanical stimuli (e.g., tension, compression) in which they are deposited and maintained (20–23).

Here, we investigate the skeletal tissues found in the PD of a previously described mature specimen of the nonornithurine ornithuromorph *Yanornis martini* from the Jehol Biota (Fig. 1) [Institute of Vertebrate Paleontology and Paleoanthropology (IVPP) V13358; preserved with impacted sand in its intestinal tract (24, 25)]. Numerous specimens preserving macerated fish remains in the stomach and either whole fish or pellets of compacted fish bone in the esophagus indicate that *Yanornis* was primarily piscivorous (24, 26). We use nondestructive high-resolution microcomputed tomography (μCT)-scanning on the whole skull, followed by multiple high-resolution analytical methods (nanoCT scanning, scanning electron microscopy [SEM], standard ground-sectioning techniques, and paraffin histology) on the extracted PD and on an extracted fragment of the right DE in order to understand the origin and function of the APD.

Results

Gross Morphology and Nondestructive μCT-Scanning. The edentulous PD in *Yanornis* IVPP V13358 is ovoid in dorsal view. In lateral view it is semicircular, such that the ventral margin is straight and the dorsal margin is strongly convex (Fig. 1). The caudal half of this convex surface articulates with the DEs (Fig. 1*A*). The right lateral half of the PD in IVPP V13358 is damaged, revealing an internal trabecular architecture (Fig. 1*B*). The left lateral surface was covered by sediments. CT scans indicate this surface was concave and perforated by 3 small foramina (Fig. 2*B*). The DEs of *Yanornis* bear numerous hypertrophied teeth (also present in the caudal portion of the PM and rostral portion of the maxilla) (26, 27). The rostral tips are unfused at the symphysis (Fig. 1). The rostral articular surface of the DEs is relatively straight and angled rostrodorsal-caudoventrally, with a slight protuberance at the rostrodorsal margin visible in lateral view (Fig. 1*B*, arrow). The DEs are perforated rostrolaterally by a large foramina, also described in *Hesperornis*, *Parahesperornis*, *Ichthyornis*, and *Jianchangornis* (7), previously identified as a ligamentous pit for the attachment of the PD to the DEs (Fig. 1*B*).

Nondestructive μCT-scanning of the skull (voxel size of 12.3 μm) reveals replacement teeth in the DEs and PM, and the mandibular canal (also known as the inferior alveolar canal) that hosts the mandibular nerve V_3 in all vertebrates (28) (third branch of the trigeminal nerve), and Meckel's cartilage during embryonic development (29) (Fig. 1*C*). Parasagittal CT slices indicate that the mandibular canal is continuous with the tooth

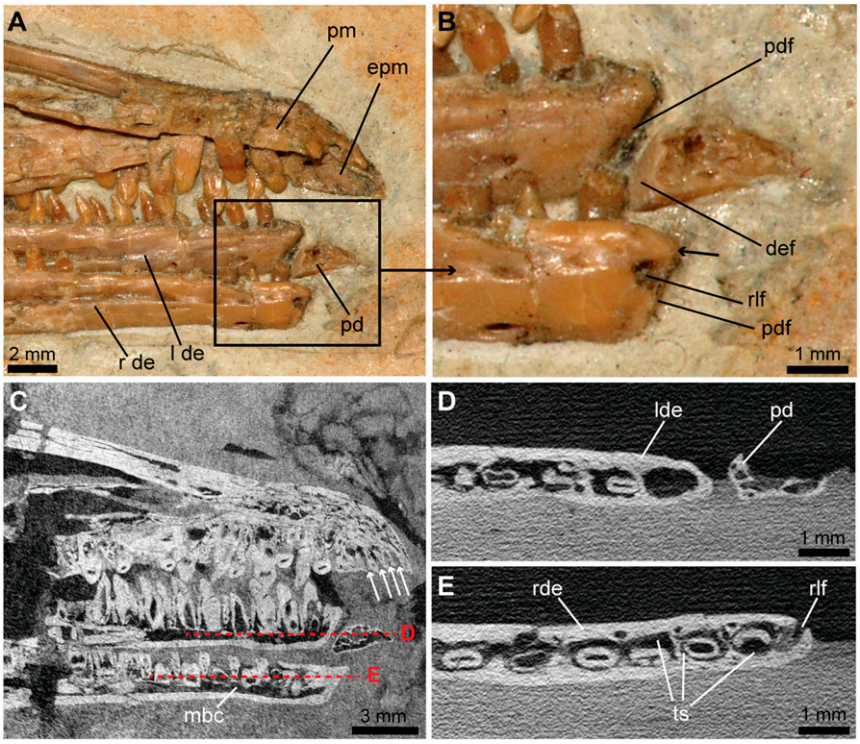

Fig. 1. Gross morphology (*A* and *B*) and μCT-scanning (*C*–*E*) of *Y. martini* (IVPP V13358). The PD is an ovoid skeletal structure located rostral to the 2 DEs, with a rostrolateral foramina. An edentulous portion of the premaxilla overlaps the PD and bears at least 4 small, dorsoventrally oriented canals, probably bearing neurovasculature (white arrows). μCT-scans show 3 main characteristics: A cancellous PD (*C*), the mandibular canal continuous with tooth sockets and the rostrolateral foramina (*C* and *E*), and a concave–convex facet between the PD and DEs (*D*). Abbreviations: def; facet for the dentary; epm, edentulous portion of the premaxilla; l de, left dentary; mbc, mandibular canal; pdf, facet for the predentary; pm, premaxilla; rde, right dentary; rlf, rostrolateral foramina; ts, tooth sockets.

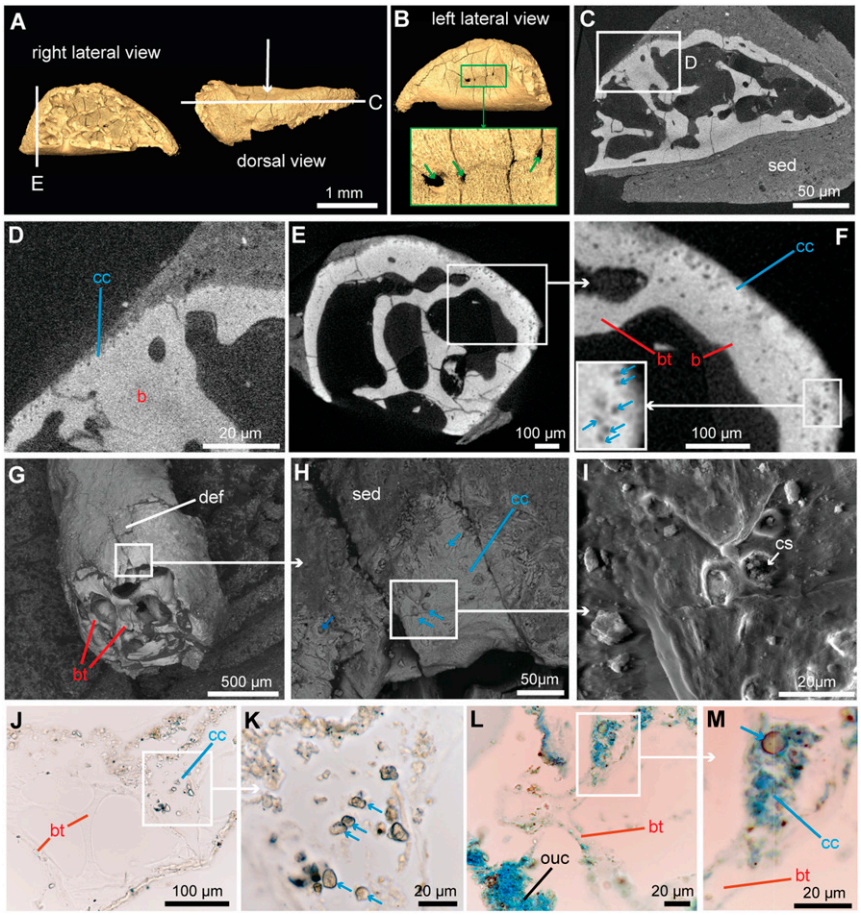

Fig. 2. Three-dimensional reconstructions (*A* and *B*), nanoCT scans (*C–F*), surface SEM (*G–I*), and paraffin sections (*J–M*) of the PD of IVPP V13358. The PD is composed of internal bony trabeculae and CC (cc) with clear chondrocyte lacunae (blue arrows in *F*, *H*, *K*, and *M*) on its caudal surface articulating with the DEs. Its left lateral side has 3 foramina (green arrows, *B*). *J* and *K* are unstained paraffin slides. *L* and *M* are adjacent paraffin slides stained with Alcian blue. The fossilized cartilage (but not the bony trabeculae, bt) reacts with Alcian blue, in a pattern consistent with extant tissues. Abbreviations: b, bone; bt; bony trabeculae; cs, calcospherites; def; facet for the dentary; ouc, originally unmineralized cartilage; sed, sediment.

sockets (Fig. 1*C*) and the rostrolateral foramina (Fig. 1*E*). The edentulous portion of the PM contains approximately 4 small, dorsoventrally oriented canals probably bearing neurovasculature (Fig. 1*C*, white arrows). Transverse slices reveal a concave articular surface on the ventral-most portion of the rostral margin of the DEs (Fig. 1*D*, visible on the left DE), suggesting a congruent concave–convex articulation between the DEs and PD.

Predentary Tissues. Nondestructive CT scans do not provide high enough resolution for specific tissue identifications (i.e., no differences in contrast between the extracellular matrices of dental tissues, alveolar bone, or PD tissues exist) (Fig. 1 *C–E*), thus we extracted the PD for higher-magnification analyses (Fig. 2). NanoCT-scanning (voxel size of 1 µm) of the extracted PD shows that it is extremely porous with thin bony trabeculae separated by large cancellous spaces most likely filled with bone marrow or neurovasculature (Fig. 2 *C–F*). A portion of the caudal articular surface is also missing, exposing some bony trabeculae (Fig. 2 *B* and *G*).

Even at extremely high resolution (1 µm), the orientation of the collagen fibers within the bone (i.e., woven, parallel-fibered, or lamellar) cannot be detected and osteocyte lacunae are not easily identifiable (Fig. 2 *C–F*). However, a thin external layer, slightly brighter than the more internal bone, with round, dark structures, is observed in many of the slices (Fig. 2 *D* and *F*). This tissue presents the characteristics of calcified cartilage (CC) with the round structures pertaining to chondrocyte lacunae (Fig. 2*F*, blue arrows). In some instances, they show a doublet pattern typical of cartilage cells that have just finished cell division (i.e., cell doublets) (30) (Fig. 2*F*).

The nanoCT scans suggest that all of this cartilage was located on the caudal articular surface facing the DEs (Fig. 2 *C–F*). Cell doublets are strong evidence for CC, but to our knowledge no previous study has reported the unequivocal appearance of this tissue in fossils using nanoCT scanning. Therefore, to confirm this preliminary identification, we employed both SEM (Fig. 2 *G–I*) and histological examinations (Fig. 2 *J–M*). SEM on the caudal articular facet closest to the DEs indeed shows round chondrocyte lacunae, including some organized into cell doublets (Fig. 2 *H* and *I*). The lacunae are filled with structures resembling calcospherites (Fig. 2*I*) previously reported in the chondrocyte lacunae of juvenile hadrosaur limb bones from Montana observed under SEM (31).

Due to the very small size of the APD and its incompleteness in IVPP V13358, acquiring a single longitudinal ground section (like that in Fig. 2*C*) using standard paleohistological methods would have been extremely challenging; therefore, we demineralized the PD and employed paraffin histology to generate more sections (5 µm thick). Longitudinal, unstained slides show bony trabeculae and peripheral cartilage with chondrocyte lacunae (Fig. 2 *J* and *K*, blue arrows). Alcian blue stain was applied to an adjacent slide (Fig. 2 *L* and *M*). In modern tissues, Alcian blue reacts with the glycosaminoglycans found abundantly in cartilage but almost absent in cortical bone (32) (*SI Appendix*, Fig. S3).

The stained slide revealed a pattern similar to extant avian bone and cartilage with the cartilage matrix staining blue and the bone matrix remaining mostly transparent, confirming our tissue identification at the chemical level (Fig. 2 *L* and *M*). The blue stain is much more intense and accumulates on the outer surface of the PD. Based on location (i.e., in continuity, or close proximity, with the CC) and chemistry (i.e., reacts positively and intensely with Alcian blue), these traces most likely represent remnants of originally unmineralized (hyaline) cartilage (Fig. 2*L*). SEM, paraffin histology (unstained slides), and histochemistry (Alcian blue-stained slides) all confirm the preliminary identification of CC based on the nanoCT data.

Dentary Tissues. In order to investigate and reconstruct the articular tissues at the PD–DE junction, we extracted the most rostral tip of the right DE of IVPP V13358, including the rostral-most tooth (Fig. 3*A*). We employed nanoCT scanning at 3 μm (Fig. 3*H*) and surface SEM (Fig. 3 *I–K*) prior to histological sampling (Fig. 3 *B–G*). Potential islands of CC were recognizable but neither individual lacunae nor cell doublets could be identified (compare Fig. 3*H* with Fig. 2*F*). Since the DE is a membrane bone (16), which are not typically associated with any cartilage in most vertebrates, additional methods were utilized in order to test this preliminary identification.

SEM on the DE fragment revealed a dark layer on the lateral surface and inside the rostrolateral foramina, and a much paler layer directly covering the articular facet, originally identified as sediment (Fig. 3 *J* and *K*). Unlike the PD (Fig. 2 *H* and *I*), this layer did not show any chondrocyte lacunae typical of CC (Fig. 3*K*). Because this DE fragment was larger than the PD, standard ground sections could easily be made (2 sections at 70 μm, both showing the same tissues) (Fig. 3 and *SI Appendix*, Fig. S4). Polarized light revealed that the rostral tip of the DE consists mostly of parallel-fibered bone, with lamellar bone closest to the tooth socket (Fig. 3*C*). A band of tissue located mostly on the medial side of the DEs (i.e., within the mandibular symphysis) (Fig. 3*C*, orange arrow; the pale layer seen under the SEM in Fig. 3*K*) and another band within the tooth socket show a similar pattern of birefringence and an orangey color under polarized light (Fig. 3*C*, orange arrows).

Higher magnification under transmitted light confirms the preliminary identification of CC based on the CT data (Fig. 3*G*). Bone is located internally and shows stellate osteocyte lacunae (Fig. 3*G*, red arrows), whereas the CC is located more externally and shows round chondrocyte lacunae (Fig. 3*G*, blue arrows).

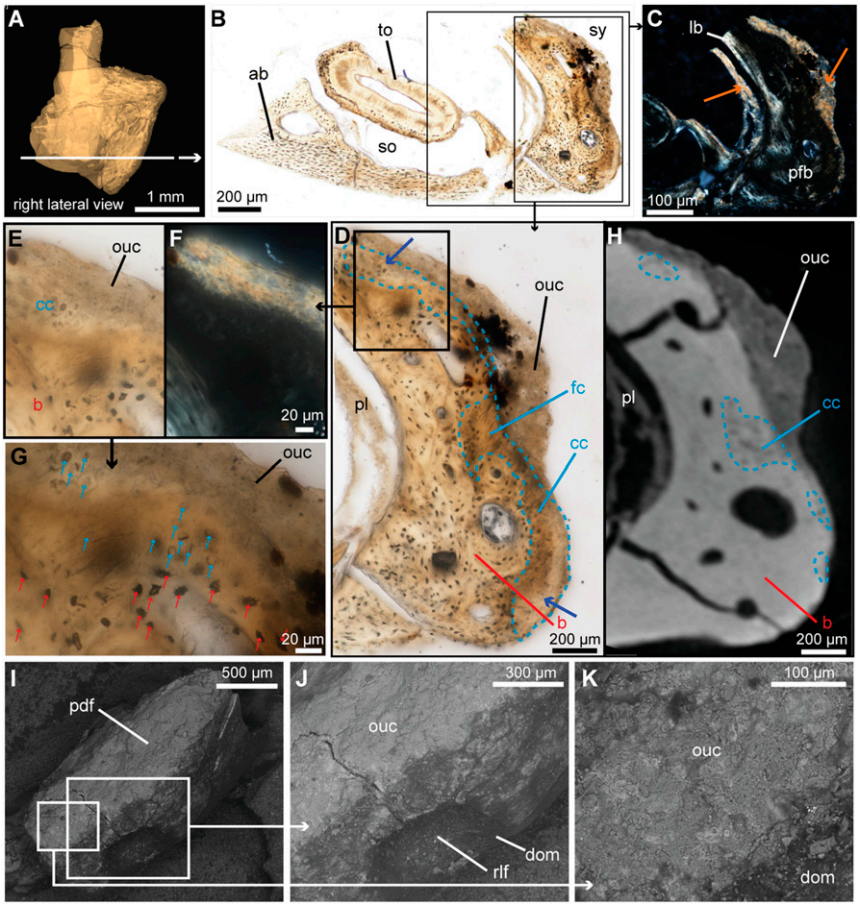

Fig. 3. Three-dimensional reconstruction (*A*), ground section (*B–D*), corresponding CT-scan (*H*), and surface SEM (*I–K*) of the right DE fragment of IVPP V13358. The rostral end and the symphyseal area of the right DE is covered by CC (cc), itself covered by potential originally unmineralized cartilage (ouc). Ground sections *B*, *D*, *E*, and *G* are shown under transmitted light. *C* and *F* are shown under the polarized light. Under the polarized light, the originally unmineralized cartilage and the periodontal ligament have an orange birefringence (orange arrows, *C*). The CC is more fibrous (fc) in the center than on the symphyseal and lateral edges (dark blue arrows, *D*). Ground sections allow clear identification of tissues and cell types: chondrocyte lacunae (blue arrows, *G*) and osteocyte lacunae (red arrows, *G*). Abbreviations: ab, alveolar bone; b, bone; dom, dark organic matter; fc, fibrocartilage; lb, lamellar bone; ouc, originally unmineralized cartilage; pdf; facet for the predentary; pfb, parallel-fibered bone; pl, periodontal ligament; rlf, rostrolateral foramina; so, socket; sy, symphysis; to, tooth. *E* and *F* are corresponding images at the same scale.

The matrix of the CC looks similar throughout the surface (i.e., laterally and near the mandibular symphysis) (Fig. 3*D*, dark blue arrows), except for 1 central area where it resembles fibrocartilage (fc in Fig. 3*D*). This is most obvious at extremely high magnification (*SI Appendix*, Fig. S5). As expected, identification of specific cell types and skeletal tissues is much more accurate with histological sections (Fig. 3*G* and *SI Appendix*, Fig. S5), but the nanoCT-scans provide a general outline of the extracellular matrix of the CC on the DE fragment (Fig. 3*H*).

The thin, external band of tissue found mostly within the mandibular symphysis (Fig. 3*C*, orange arrow on the right) is continuous with the CC and no clear demarcation between the 2 tissues can be determined either histologically (Fig. 3 *D*–*G*) or chemically using energy-dispersive spectroscopy (EDS) analysis (*SI Appendix*, Fig. S6). EDS suggest that this layer is organic and its continuity with the CC suggests it is a remnant of originally unmineralized cartilage, most likely similar to that found on the PD (Fig. 2*L*). Potentially, it may also involve some of the dense connective tissues (such as collagen fibers) originally part of the mandibular symphysis. EDS analysis of the fibrous tissues found within the tooth socket also suggest they contain organic remains (*SI Appendix*, Fig. S7), and their location indicates they are remnants of the periodontal ligament (pl in Fig. 3 *D* and *H*).

Three-Dimensional Skeletal Tissue Reconstructions on the Predentary and Dentary. The nanoCT-data were used to generate a 3D model showing the distribution of bone and CC on the PD and DEs of *Yanornis* (Fig. 4). On the PD, cartilage is present caudally where it articulates with the DEs and is not found internally within the bony trabeculae nor on the rostral surface. We refer to this as the "articular cartilage" of the PD (Fig. 4*B*). On the DE, 3 distinct patches of CC are identified: 2 symphyseal patches, which we refer to as the dorsal and ventral symphyseal cartilages, and 1 rostral articular patch directly facing the PD, which we refer to as the rostral articular cartilage (Fig. 4 *B* and *C*).

Specific Cartilage Identification on the Predentary and Dentary. The 2 main types of cartilage found within the modern avian cranium are: 1) Primary cartilage found within endochondral elements (i.e., as remnants of the cartilaginous anlagen), or at their ends covering the epiphyses (i.e., as articular cartilage); and 2) secondary cartilage (SC) directly arising on membrane bones, such as the DEs (33). Avian SC arises after bone formation directly from the periosteum (33). SC can be found at ligamentous attachments or directly within cranial joints (within synovial, kinetic joints) as articular cartilage (33–35). Because the DE is a membrane bone, the 3 patches of cartilage on the DE of *Yanornis* (Figs. 3 and 4) are SC. This report of SC in a fossil bird is unique. Whether the articular cartilage present on the PD of *Yanornis* (Figs. 2 and 4) is primary or secondary can only be determined once the developmental origin of the PD is understood, which we discuss below.

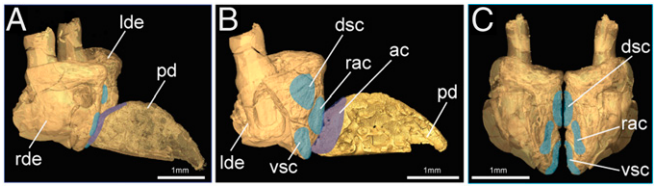

Fig. 4. Three-dimensional and skeletal tissue reconstructions of the PD and DEs in lateral-oblique (*A*), symphyseal (*B*), and rostral views (*C*). The PD has articular cartilage (ac) on its caudal end. The DEs have a rostral articular cartilage (rac), a dorsal symphyseal cartilage (dsc) and a ventral symphyseal cartilage (vsc), which are all secondary cartilages because the DEs are membrane bones.

Discussion

Twenty-first century paleontology is increasingly becoming a biological science, firmly rooted in our understanding of extant tissues. Investigating the origin of skeletal novelties is facilitated through direct observation of homologous processes in living species [e.g., embryonic fate-mapping, and whole-mount staining of ossification centers (36, 37)]. However, our understanding of the APD is hindered because no comparable structure is present in extant amniotes. In neornithines, a PD has been hypothesized to be present in the recently extinct neognathous *Teratornis merriami* (38) and a few Cenozoic birds have been reported with intersymphyseal structures (*SI Appendix*, Table S1 and references therein). However, the poor preservation of these elements makes it impossible at this time to explore potential homology with the APD of nonneornithine ornithuromorphs. Although some extant istiophorid fish have a structure referred to as a PD (*SI Appendix*, Fig. S8), both the phylogenetic distance between the Ornithuromorpha and Istiophorida, and the fact that the PD of istiophorids sometimes has teeth or denticles (3), indicate that embryological data collected from these extant teleosts is unlikely to be comparable or informative to the development of the (presumably) nonhomologous APD.

Examination of the preserved PD and DE tissues in *Yanornis* allow us to better understand the origin and function of this avian evolutionary novelty. Although this study utilizes a diverse array of analytical methods at various resolutions (Figs. 1 and 3), our results indicate accurate identification of skeletal tissues requires histological examination through standard ground sections (or paraffin sections) combined with extremely high-resolution nanoCT scans (≤1 μm). μCT-scanning of IVPP V13358 (Fig. 1) and other specimens of nonornithurine ornithuromorphs preserving a PD (*SI Appendix*, Fig. S9) did not provide enough resolution to allow specific tissue identification. Combined histology and nanoCT data allow us to provide interpretations regarding the soft-tissue forming the rostral ends of the jaws of *Yanornis* and to propose a mechanism for the evolution of the APD in a wider phylogenetic context.

Developmental Hypotheses for the Predentary of *Yanornis*. We have proposed 3 possibilities for the developmental origin of the APD. Here we explore each possibility and demonstrate that the current evidence most strongly supports identification of the APD as a sesamoid bone (developmental hypothesis 3).

Developmental hypothesis 1: Origin within the dermatocranium. Based on the tissues preserved in IVPP V13358, 1 plausible interpretation is that the PD arises directly as bone from the cephalic mesenchyme via intramembranous ossification, from a single or paired ossification center originally part of the DEs. Such a process would represent an exostosis of dermal cranial bones (39). This type of origin has been proposed for the PD in different clades of fossil fish (Ichthyodectids and Aspidorhynchids), although these hypotheses were not accompanied by any supporting microscopic data (1–3). After ossification, SC on the caudal surface of the PD would then arise from the periosteum, as commonly occurs in extant birds (33–35).

In IVPP V13358, the PD consists of trabecular bone (Fig. 2) with articular cartilage located solely on its caudal surface where it articulates with the DEs (Figs. 2 and 4). We found no remnants (islands) of CC internally within the bony trabeculae to clearly indicate that this structure originated as cartilage. However, because IVPP V13358 is a fairly skeletally mature specimen (based on its size and gross morphology), without a much younger specimen of *Yanornis* we cannot rule out the possibility that the articular cartilage seen in IVPP V13358 is not a remnant of earlier ontogenetic stages. It is still possible the PD of the skeletally mature IVPP V13358 first formed as cartilage and was almost completely replaced secondarily by bone via endochondral ossification, except

on the caudal-most surface. In this case, the "leftover" articular cartilage would not represent SC, but primary cartilage instead.

This scenario, in which the PD in *Yanornis* forms first as a cartilaginous structure, represents hypotheses 2 and 3 in which: 2) the cartilage could form from chondrification centers derived from the 2 rods of Meckel's cartilage, which then would become fused into an unpaired structure and ossify; or 3) the cartilage could come from 1 (or more) chondrification centers forming directly within the dense connective tissues rostral to the DEs. In this last case, the PD of *Yanornis* would be characterized as a sesamoid.

Developmental hypothesis 2: Origin within Meckel's cartilage. Ontogenetic processes in extant taxa provide information regarding potential developmental pathways through which the APD could arise from Meckel's cartilage. Extant birds have been reported as having transitional "mentomandibular bones" (sometimes synonymous with "mentomeckelian bones") derived from the rostral ossification of Meckel's cartilage present only during early ontogeny (15, 40–42). These mentomandibular bones could represent an atavism, potentially forming the unfused precursors of a PD element. Such an origin has been hypothesized for the PD in ornithischian dinosaurs although, again, this hypothesis relied solely on gross morphology (4). However, closer inspection of the literature indicates it is unlikely that the PD in *Yanornis* (and other nonneornithine ornithuromorphs) is derived from Meckel's cartilage because the mentomandibular bones (40–42) reported in modern birds do not exist to our knowledge, and they may in fact be recent misinterpretations of older literature and embryological descriptions (*SI Appendix*, *Supplementary Text 1*). In addition to referring to the anterior ossification of Meckel's cartilage (Plate 101 in ref. 15), other authors have referred to mentomandibular bones as the rostral-most intramembranous ossification centers of the DEs (e.g., refs. 43 and 44) (*SI Appendix*, *Supplementary Text 1*). No current data support the existence of separate mentomandibular bones derived from Meckel's cartilage in neornithines, even as transitory ontogenetic structures. They are not separate bones of the lower avian jaws; in one reference they represent the ossification of Meckel's cartilage (15), and for others they represent membranous ossification centers that are part of the DEs (e.g., refs. 43 and 44 and *SI Appendix*, *Supplementary Text 1*).

It has recently been demonstrated that the 2 rods of Meckel's cartilage can persist late into avian ontogeny, even through subadulthood in some paleognaths [the ostrich and the emu (29; in contrast to refs. 45 and 46)]. A potential remnant of "degenerative" Meckel's cartilage has also been reported in an adult duck (35). However, the rostral-most ends of Meckel's cartilage do not meet nor do they fuse into any type of rostral structure in these species, nor was evidence of fusion ever found in quail and duck embryos or duck hatchlings (35, 47). In the American alligator, Meckel's cartilages fuse in the midline and persist through adulthood, but similar to Neornithes, they do not take part in any rostral structure and simply stay embedded within the 2 dermal DEs at the mandibular symphysis (48). A survey of the literature including more remote outgroups (*SI Appendix*, Table S1) also fails to identify strictly rostral, unpaired structures derived from Meckel's cartilage.

Because there is no evidence of any rostral structure nearing or anterior to the symphysis originating from Meckel's cartilage in modern birds and crocodilians (and other outgroups), we find no basis for formulating a convincing developmental hypothesis involving Meckel's cartilages (in contrast to ref. 41), and presumably their fusion into a single unpaired structure in the formation of the APD.

Developmental hypothesis 3: A sesamoid of ectocranial origin. Sesamoids are small, ovoid nodules of cartilage or bone that arise outside of the skeleton (i.e., ectocranial) within a continuous band of regular dense connective tissue that wraps around or is near a bony prominence (18, 49). They are very common in all amniotes and mostly documented in the postcranium [e.g., the patella, the meniscus (50)]. However, sesamoids are also known to form near the skull (49); the North Island Kokako has 3 sesamoids near its craniomandibular joint, and many nocturnal birds (at least 10 species of owls, and the Common Potoo) possess a sesamoid in their sclera that helps contract the nictitating membrane (51, 52).

Sesamoids all arise from a chondrification center and may or may not be replaced with bone through endochondral ossification (49). After bone replacement has ceased, these elements often show the same bony architecture as that of the normal skeleton [e.g., with trabecular, cancellous bone, and even bone marrow (18)]. Sesamoids can even have articular cartilage on surfaces that articulate with other nearby bones (e.g., refs. 18, 50, 52, and 53). The PD of *Yanornis* possesses all of these characteristics: It is an ovoid structure located near a bony prominence (the DEs); found within connective tissues (Fig. 1); consists of trabecular bone; and has articular cartilage on the surface that directly faces the DEs (Figs. 2 and 4). All of these characteristics are consistent with the possibility the APD is a sesamoid. The presence of cartilage rules out identification of the APD as a type of osteoderm or ossified tendon (structures that also arise ectocranially within connective tissues), as they do not possess nor develop articular cartilage at any time during ontogeny in extant species (54, 55). Osteoderms in all extant sauropsids arise within the dermis, which has an osteogenic potential [referred to as a "deep homology" (56)] but lacks a chondrogenic potential (54, 57).

The location of the APD at the rostral-most tip of the lower jaws further supports possible identification as a sesamoid: The rostral regions of the jaws of extant birds (and other vertebrates) are often subjected to high amounts of mechanical stress—such as those related to foraging, feeding, food manipulation, or nest building (58)—and mechanobiological stimuli are the main factors contributing to the formation of sesamoids in extant birds [although exceptions exist (18)]. The development of most sesamoids derives from the capacity of connective tissues to alter their cellular structure, cell secretions, tissues types, and genetic expression patterns in direct response to changes in the mechanical loading environment (18). There is strong evidence that sesamoids are a physiological and evolutionary adaptation of connective tissues in response to compressive forces (18, 59). Based on the mechanobiology of extant sesamoids, identification of the PD as such an element would suggest that compressive forces within the connective tissues located rostral to the DEs in *Yanornis* were involved in the formation of a cartilaginous sesamoid. This hypothesis is further supported by the presence of SC on the DEs of *Yanornis*. The mechanobiology of avian SC (22, 34, 60–62) suggests that the predominant force acting between the PD and DEs in *Yanornis* was compression.

Evidence for Compression at the Predentary–Dentary Junction. Cartilage in all vertebrates (whether it is primary or secondary) is a tissue that resists compression and absorbs shock due to its unique chemistry, differing strongly from that of bone, which is more resistant to tension (20, 63, 64). Our analyses identified articular cartilage on the PD directly facing a patch of secondary articular cartilage on the DEs (the rostral articular cartilage) (Fig. 4). In the extant avian cranium, SC arises due to compression and/or shear, but not tension (22, 34, 60–62). When compression and/or shear is artificially applied to the periosteum of avian membrane bones, the osteoprogenitor cells switch from osteogenesis to chondrogenesis (22, 60, 61, 65). In developing chicken embryos, already-formed (preexisting) SC cannot be maintained in the absence of these mechanical stimuli (22). In the absence of stimuli, it is resorbed or transformed into bone (22). Therefore, with the assumption that the SC of Mesozoic birds shared the same mechanisms of induction and maintenance as that of their living relatives, the presence of SC on the DEs

(i.e., the rostral articular cartilage) (Fig. 4) of *Yanornis,* directly facing the caudal articular surface of the PD, can only be explained by compressive forces. These compressive forces were most likely generated by some mobility of the PD.

Evidence of Kinesis at the Predentary–Dentary Junction. Inferences regarding some form of mobility or kinesis at the rostral tip of the lower jaws in *Yanornis* is not unreasonable; many modern birds are characterized by a high degree of flexibility in their bills [e.g., prokinesis, rhynchokinesis, distal rhynchokinesis (66–68)]. Kinesis at the DE–PD junction in *Yanornis* has already been hypothesized by Zhou and Martin (7), potentially as an adaptation to facilitate gape because this feature is reminiscent of the intraramal joint of some extant piscivorous birds (*SI Appendix*, *Supplementary Text 2*). In fact, the SC found on the DEs on *Yanornis* is not only an indicator of compression, but we argue that it is also an indicator of joint movement (69), which in turn suggests the APD may have increased foraging efficiency or precision.

Studies on the mechanobiology of SC in the heads of extant birds are crucial for inferences of joint movement in the skulls of Mesozoic birds. Although tissues bearing the same name are described in mammals and teleosts, these 3 occurrences represent cases of convergent evolution and their mechanisms of maintenance are different (33, 35, 70, 71). Currently, avian SC is not found in other extant sauropsids. However, it has been found in hadrosaur crania, indicating this "avian" tissue evolved much earlier in the Dinosauria, far preceding the origin of birds themselves (71). SC can be found as articular cartilage on membrane bones in kinetic joints in neornithine crania (34, 35). In addition to showing that SC arises mostly under compressive forces (22, 34, 60–62), other experimental studies on the heads and cranial joints of developing chicken embryos have shown SC does not form during paralysis, unlike primary cartilage, which forms both under normal and paralyzed conditions (21, 22, 65). Paralyzing agents inhibit muscle contractions and associated cranial joint movements, such as beak-clapping [that occurs during normal embryonic development (72 and 73)]. These earlier studies artificially transformed mobile joints into immobile joints and showed that avian SC cannot form, nor be maintained without some type of movement, and concluded that mechanical stimuli and physical movement [i.e., active movement (23)] directly within the joint are responsible for SC formation (21).

During the normal development of the skull, most mechanical stimuli come from joint movement (i.e., active movement) (23). Most of the kinetic joints of modern birds (involving membrane bones) that have been investigated histologically possess SC [in the chicken, the Eastern rosella, the Mallard duck (34, 35, 74)]. Therefore, based on both mechanobiological and histological studies of SC in avian cranial joints, it is safe to infer that the SC found on the DEs of *Yanornis* indicates mobility at the DE–PD joint. Inferences of movement based on tissue type (i.e., presence of SC) at this time cannot shed light on the exact type of joint movement, nor provide a precise quantification of movement as no standardized method of quantification during embryonic development yet exists (75). However, it is safe to infer that translation/compression of the PD on the DEs was at least possible, with potential for some ventral movement (even if very slight). This ventral flexion is suggested by the articular cartilage found covering the entire articular surface of the PD, which is round and convex, and fits well into the concave facets made by the DEs. Zhou and Martin (7) hypothesized that the DEs and the PD in *Yanornis* were linked by a kinetic, synovial joint, and several lines of evidence indicate that this remains a reasonable inference for this joint structure at this time.

Joint Structure Hypotheses. Synovial joints in extant vertebrates are typically mobile and in the heads of living birds they are the main types of joint that allow cranial kinesis (35). Avian synovial joints possess articular cartilage (either primary or secondary) on each side of a synovial cavity filled with lubricating fluid, all surrounded by a fibrous capsule. Because of the mobility of synovial joints, they are typically congruent with concave–convex morphologies between their articular surfaces. The PD in *Yanornis* is located at the very tip of the lower jaws, has a convex articular surface that fits into a concave articular surface on the DEs (Fig. 1*D*), and possesses articular cartilage that directly faces the rostral articular cartilage of the DEs (Fig. 4). Morphological, histological, and topographical data together support the possibility of a synovial joint between the PD and the DEs of *Yanornis* (Fig. 5). This type of joint would necessitate strong stability between the DEs (in order for the synovial cavity and capsule to not get ripped).

It is not uncommon for avian sesamoids to be found within or near a synovial cavity (18, 49). However, because close-fitting, concave–convex joints in extant sauropsids do not always have a synovial cavity and may instead show articular cartilage linked by collagen fibers (70), and because no clear osteological nor histological correlate of a synovial cavity or fibrous capsule has ever been clearly identified in the cranial synovial joints of extant birds, the possibility of a mixed cartilaginous–fibrous joint between the PD and DEs of *Yanornis* cannot be ruled out at this time (*SI Appendix*, Fig. S10). Nevertheless, even though there are 2 possibilities regarding the structure of the PD–DE joint in *Yanornis* (Fig. 5 and *SI Appendix*, Fig. S9), our histological data completely rules out the possibility of a fibrous joint (i.e., a suture) like that found at the junction between the DEs and the PD in a Pacific sailfish (*SI Appendix*, Fig. S8). To our knowledge, the PD of istiophorid fish is a very stable structure and no movement for this bone has been reported. The lower jaws in these fish have been described as adapted for speed, and the extension of the lower jaws has been hypothesized to facilitate this speed-efficient jaw system during prey capture (76, 77). This stable system may explain (at least partially) the differences in joint structure compared to *Yanornis*, and the complete absence of cartilage in istiophorids (*SI Appendix*, Fig. S8). Although *Yanornis* was piscivorous (26), it lacks postcranial modifications associated with plunge-diving, and it most likely fished while wading in the shallow waters of lakes (*SI Appendix*, *Supplementary Text 2*). The APD persisted for 60 My and was most likely not strictly associated with a piscivorous diet. It is also found in some ornithuromorphs (i.e., *Gansus*, *Hongshanornis*, *Iteravis*) preserving gastroliths, commonly

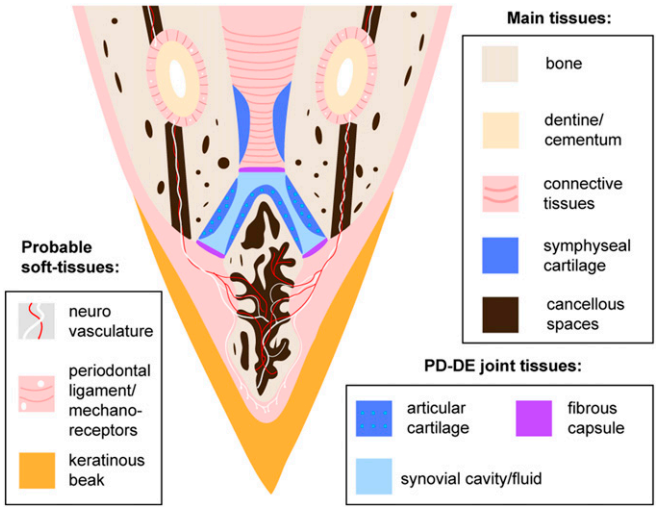

Fig. 5. Schematic representation of a hypothetical horizontal section through the anterior lower jaws of *Yanornis* showing the main joint tissues and other soft-tissue interpretations.

found today in birds that eat tougher material, such as seeds or insects (26).

In extant vertebrates, separate (unfused) DEs at the mandibular symphysis are always linked in their midline by dense connective tissues (35, 48, 78), but may also involve some symphyseal SC nodules in mammals (79, 80) similar (but not homologous) to those seen in *Yanornis*. Based on these neontological histological studies, a mixed cartilaginous–fibrous joint is the only possible interpretation for the mandibular symphysis of *Yanornis* (Fig. 5). This differs from the mandibular symphyses of some young hadrosaurs, which have chondroid bone within their DEs (81) instead of nodules of SC.

Soft-Tissue Interpretations and Strong Evidence for a Proprioceptive Predentary. Nondestructive μCT-scans indicate that the mandibular canal hosting the mandibular nerve V_3 is continuous with the tooth sockets and with the rostrolateral foramina (Fig. 1*E*). Originally identified as a pit for the insertion of a ligament linking the DEs into a small depression on the PD [seen in *Yanornis* and *Hesperornis* (7)], CT scans (Fig. 1), histology (*SI Appendix*, Fig. S4), and data on extant crocodilian teeth (82) suggest an alternative interpretation. To our knowledge, there is no extant example of external ligaments that penetrate tooth sockets and are continuous with the periodontal ligament and no histological evidence of ligamentous attachment (Sharpey's fibers) can be seen in the ground section cut through the foramina (*SI Appendix*, Fig. S4). Instead, the most plausible interpretation is that the foramina is the exit point of vasculature and nerves coming directly from the mandibular canal. This pit could be renamed "rostrolateral neurovascular foramina." The neurovasculature originating from the DEs most likely entered the PD through the 3 lateral foramina observed on the left surface (Fig. 2*B*) and allowed transmission of sensory and proprioceptive information between the PD and the rest of the skull.

Additionally, because the mandibular canal was apparently continuous through the entire tooth row (Fig. 1 *C* and *E*), it is plausible to conclude that the teeth of *Yanornis* were proprioceptive and able to receive biomechanical information, similar to the teeth of *Caiman sclerops*, in which the periodontal ligament is filled with nerve endings and mechanoreceptors (82). Compared to the plesiomorphic avian condition, the teeth in *Yanornis* are hypertrophied (26) but whole fish have been found in the crop of many specimens, suggesting *Yanornis* did not utilize its teeth to process food prior to ingestion, but used them solely for prey capture (24). Our data suggest that prey capture may have been facilitated by a highly proprioceptive dental system involving both richly innervated teeth (i.e., with possible receptors within the periodontal ligament) and a richly innervated PD. However, because neither the PD nor the DEs in *Yanornis* are strongly pitted (Figs. 1 *A* and *B* and 2), it may not be exactly comparable to the extant specialized "bill tip organ" found in some highly proprioceptive birds (e.g., probe-foraging, fish-eating birds like sandpipers and ibises) that possess innumerable pits/foramina filled with mechanoreceptors on their DEs and PM (83). Proprioceptive rostra clearly evolved multiple times within Aves.

In ibises, clusters of mechanoreceptors have been reported in the rostral-most dermis of their beaks, but they lack osteological correlates because they are not directly associated with a bony sensory pit (84). Therefore, we cannot rule out the possibility that *Yanornis* also had some mechanoreceptors coming directly from the mandibular nerve embedded within the dermis surrounding the PD (Fig. 5), enhancing the proprioceptive abilities of this system. Proprioception (e.g., remote-tactile sensory systems) facilitates prey detection in probe-foraging birds in shallow waters (e.g., Scolopacidae and Threskiornithidae) or in the substrate on land (e.g., kiwi) (83, 84). In these extant birds, the bill tip organ is covered by a keratinous rhamphotheca (83) and we argue that this was most likely also the case in *Yanornis*.

Possibility of a Rhamphotheca. The presence of a rhamphotheca in *Yanornis* cannot be safely assessed by the presence of bony pits or foramina as they are not reliable characteristics for modeling keratinous sheaths in fossils at this time (e.g., ref. 85, contra ref. 86). Instead, the major line of evidence supporting the presence of a rhamphotheca comes from the edentulous portion of the PM that dorsally articulates with the PD (Fig. 1*A*). This association has been noted not only in *Yanornis* but in all other ornithuromorphs with a PD (7).

Odontogenesis is inhibited by beak formation in ovo in extant birds (28, 87), leading to the hypothesis that the truncation of odontogenesis in fossil dinosaurs and birds corresponded with expansion of rostral keratin, which together drove the evolution of edentulous beaks (28). The absence of teeth at the rostral tip of the PM in *Yanornis* may indicate that a keratinous sheath had already started to form. CT scans reveal 4 dorsoventral canals in the PM, which may be related to a keratinous sheath, and/or our hypothesized proprioceptive system.

In the Ornithuromorpha, tooth loss apparently started in the rostral-most part of the PM and later extended onto the maxillae and the DEs (87). Because the Mesozoic APD is always associated with an edentulous portion of the PM overlapping the PD, these 2 structures most likely coevolved. No PD has ever been found bearing teeth and no vestigial alveoli are visible in the CT scans in IVPP V13358. Therefore, it is possible that the PD was covered (at least partially) by a keratinous sheath (Fig. 5) matching that on the edentulous portion of the PM. Together, the edentulous portion of the PM and the PD may represent a unique strategy in which a small beak coexisted with teeth, and notably, a PD has never been identified in an edentulous Mesozoic bird. Although the PD is only found in nonneornithine ornithuromorph birds and was consequently lost in crown birds (6), this feature persisted in Cretaceous ornithuromorphs for ∼60 My. In the future it may be possible to confirm the presence of a beak through direct evidence of soft-tissues (87), although preservation of the rhamphotheca is rare in the fossil record (26).

Toward a Synthesis and a Model: Proposed Mechanisms for the Origin, Structure, and Function of the Mesozoic Avian Predentary. The APD is an enigmatic bone, apparently a common feature of early nonneornithine ornithuromorphs that persisted for ∼60 My before it was subsequently lost, probably during the taxonomic bottleneck caused by the end Cretaceous mass extinction (6). It is unlikely that this structure had a dermatocranial or splanchnocranial origin; instead, it may have arisen from connective tissues due to the evolutionary ability of integument to easily alter its genetic expression and cellular secretions under biomechanical stimuli, contributing to the formation of new skeletal structures (18, 57). Sesamoid morphogenesis is a perfect example of balance between genetic and epigenetic controls (18, 23, 88). It would be too speculative to hypothesize where the original compressive forces that first triggered the formation of a PD in Mesozoic birds came from. In extant birds, the tip of the bill is used for a variety of tasks, such as pecking, probing, preening, or nest building (58), all of which can generate compressive forces. The APD evolved in the absence of a fused mandibular symphysis, and may represent an alternative pathway to dealing with the forces experienced by the rostral-most portion of the lower jaw.

It is clear that the evolution of the PD cannot be understood if studied in isolation. It was closely linked to other skeletal and soft-tissue structures, evolving through a complex interplay between natural selection and other evolutionary mechanisms. Notably, the APD probably coevolved with the edentulous portion of the PM, and represents a unique adaptation utilizing both rhamphotheca and teeth. The beak is one of the most diverse and plastic structures produced during avian evolution, and the morphology of the APD adds to the huge diversity of recognized

beak morphologies and kinetic strategies (58, 87). Cranial kinesis is a feature of all neornithines (66), but based on anatomical features [e.g., postorbital bar, or robust craniofacial hinge (e.g., ref. 89)], it is commonly inferred that kinesis was less prominent in Cretaceous birds. A recent study suggests that cranial kinesis evolved within the Neornithes as a feature of the Neognathae (90). Accurate inferences of kinesis are difficult, but our investigation suggest at least one extinct form of kinesis was present in the lower jaws of Cretaceous ornithuromorphs, similar (but opposite) to the distal rhynchokinesis seen in the upper beak of some extant shorebirds, which improves their foraging efficiency (68).

In *Yanornis*, strong evidence suggests that the PD was both proprioceptive and kinetic, aiding this species as it was foraging for fish in the shallow parts of the Jehol lakes (near the lakeshores). Together, proprioception combined with kinesis may have played a role in prey detection and in increasing the dexterity and precision of the tip of the jaws during foraging and food manipulation (*SI Appendix*, *Supplementary Text 2*), representing a previously undocumented and now extinct form of avian cranial kinesis. Although *Yanornis* was a piscivore, we do not draw a link between the APD and this diet. The APD was present in Cretaceous ornithuromorphs with a variety of dental arrangements, rostral proportions, and body shapes, including some taxa preserving gastroliths (26). As more extant and fossil birds are investigated, a deeper understanding of the APD will precipitate and help refine the functional and developmental hypotheses proposed here; still, this current study utilizing numerous advanced analytical methods sheds considerable light on the evolution of one of the most enigmatic known elements of avian evolution.

Materials and Methods

Whole-Skull μCT-Scanning. The skull of IVPP 13358 (Fig. 1) was μCT-scanned with an industrial CT scanner Phoenix v|tome|x. CT scans with a voxel size of 12.3 μm were observed and visualized using the software VGSTUDIO MAX (2.0). The skulls and predentaries of 3 other nonornithurine ornithuromorphs were also CT-scanned with a 160-Micro-CL (Computed Laminography) at the IVPP (Beijing China), but the resolution did not allow accurate skeletal tissue identification, such as that of cartilage (*SI Appendix*, Fig. S9).

SEM on Extracted Fragments. The PD and a fragment of the right DE of IVPP 13358 were extracted from the skull, and their articular surfaces were analyzed using SEM at the Chinese Academy of Geological Sciences with a FEI Quanta 450 (FEG) at 20 kv (Figs. 2 and 3). Prior to this, the fragments were rapidly etched in 10% acetic acid for better cartilage visualization (31). Both backscattered electrons and secondary electron modes were applied.

NanoCT-Scanning and Segmentation of the Fragments. The PD and fragment of DE of IVPP 13358 were scanned at extremely high resolution on a Phoenix nanotom at, respectively, 1 μm and 3 μm (91). CT-scans were observed and visualized using the software Avizo (v9). The CC on each bone was segmented using the segmentation tool in this software and 2 3D renderings, showing cartilage distribution were generated (*SI Appendix*, Fig. S11). For visual purposes, we manually added the different CC patches (based on *SI Appendix*, Fig. S11) using the software Adobe Illustrator CC 2018 on images of these 3D models (Fig. 4). The 3D model of the right DE was mirrored to generate a left DE, and the 3 models of the DEs and PD were combined into 1 file. The PD was placed rather ventrally on the DEs based on the location of the concave articular surface seen in the μCT scans (Fig. 1 *C* and *D*).

Demineralization, Paraffin Histology, and Histochemistry. Three samples were demineralized (*SI Appendix*, *Supplementary Text 3*) and subjected to paraffin histology: The entire PD of IVPP 13358 (Fig. 2 *J*–*M*), a piece of subchondral bone and articular cartilage from the femur (at the knee joint) of an extant passerine (house sparrow, species indet) (*SI Appendix*, Fig. S3), and a fragment of PD and DE of a Pacific sailfish (species undetermined) donated to IVPP by a private collector (*SI Appendix*, Fig. S8). Extant tissues were fixed in 10% neutral buffered formalin for 48 h prior to demineralization. All tissues were then subjected to routine dehydration, to clearing in xylene, and to paraffin infiltration and embedding (*SI Appendix*, *Supplementary Text 3*). Sections were cut at 5 μm on a rotary microtome (Leica Biosystems RM2265), placed in a warm water bath at 44 °C with section adhesive (Tissue-Grip, StatLab), mounted on charged slides (Superfrost Plus, Fisher Scientific), then dried in an oven at 60 °C for 1 h. Some finished slides of IVPP 13358 were left unstained (Fig. 2 *J* and *K*): They were simply deparaffinized in different solutions of xylene for about 15 min and cover-slipped with mounting medium (Permount, Fisher Scientific).

Alcian blue stain commonly used to differentiate cartilage from bone in extant materials (92) [e.g., the passerine (*SI Appendix*, Fig. S3)] was applied to some slides of IVPP 13358 (Fig. 2 *L* and *M* and *SI Appendix*, Text 3). Masson's trichrome (93) (*SI Appendix*, *Supplemental Text 3*), a general connective tissue stain, was applied for the Istiophorid PD for a better visualization of the tissues (*SI Appendix*, Fig. S8; since it did not present cartilage, Alcian blue is not the appropriate stain in this case).

Paleohistology-Petrographic Ground Sections of the DE Fragment. The fragment of DE was embedded in EXAKT Technovit 7200 1-component resin and cured for 24 h. Two sections (Fig. 3 and *SI Appendix*, Fig. S4) were cut using an EXAKT 300CP accurate circular saw, and then ground and polished using the EXAKT 400CS grinding system until the desired optical contrast was reached around 70 μm. Sections were observed under natural and polarized light using a Nikon eclipse LV100NPOL, and photographed with a DS-Fi3 camera and the software NIS-Element v4.60. Paraffin sections were observed and photographed with this same system. We used the Photomerge tool in Adobe Photoshop CS6 to reconstruct the entire sections.

Additional SEM and EDS on a Ground Section. SEM was performed directly on 1 petrographic ground section (same previous settings) (*SI Appendix*, Fig. S6), the EDS profile was measured as a line, continuous between the CC and the potential unmineralized cartilage, and in between the bone the potential remnant of periodontal ligament (*SI Appendix*, Fig. S7). This was done as means to preliminarily test (although it is a nonspecific test) if these soft tissues potentially had organic remains.

ACKNOWLEDGMENTS. We thank Zhang Limin for facilitating lab access; Pengfei Yin for computed tomography scanning; Dahan Li and Xinzheng Liu for extracting the bone samples; Shukang Zhang for sectioning the dentary; Hua Xiang for scanning electron microscopy and energy-dispersive spectroscopy access; Jing Lu for acquiring the fish specimen; and Josef Stiegler and Aaron Leblanc for interesting discussions. This work has been supported by the Chinese Academy of Sciences–President's International Fellowship Initiative program; the Craton destruction and terrestrial life evolution program of the National Natural Science Foundation of China (Grant 41688103); and the Strategic Priority Research Program of the Chinese Academy of Sciences (Grant XDB26000000).

1. P. M. Brito, Révision des Aspidorhynchidae (Pisces, Actinopterygii) du Mésozoïque: Ostéologie, relations phylogénétiques, données environnementales et biogéographiques. *Geodiversitas* **19**, 681–772 (1997).
2. D. Bardack, G. Sprinkle, *Morphology and Relationships of Saurocephalid Fishes* (Field Museum of Natural History, 1969).
3. H. L. Fierstine, S. P. Applegate, Billfish remains from southern California with remarks on the importance of the predentary bone. *Bull. South. Calif. Acad. Sci.* **67**, 29–39 (1968).
4. J. Ferigolo, M. C. Langer, A Late Triassic dinosauriform from south Brazil and the origin of the ornithischian predentary bone. *Hist. Biol.* **19**, 23–33 (2007).
5. S. Zhou, J. K. O'Connor, M. Wang, A new species from an ornithuromorph (Aves: Ornithothoraces) dominated locality of the Jehol Biota. *Chin. Sci. Bull.* **59**, 5366–5378 (2014).
6. Z. Zhou, F. Zhang, Discovery of an ornithurine bird and its implication for Early Cretaceous avian radiation. *Proc. Natl. Acad. Sci. U.S.A.* **102**, 18998–19002 (2005).
7. Z. Zhou, L. D. Martin, Distribution of the predentary bone in Mesozoic ornithurine birds. *J. Syst. Palaeontology* **9**, 25–31 (2011).
8. L. Martin, "The beginning of the modern avian radiation" in *Documents des Laboratoires de Géologie de Lyon* , C. Mourer-Chauviré, Ed. (Université-Bernard, Villeurbanne, 1987), **vol. 99**, pp. 9–19.
9. W. K. Gregory, G. M. Conrad, *The Comparative Osteology of the Swordfish (Xiphias) and the Sailfish (Istiophorus)* (American Museum of Natural History, 1937).
10. J. K. O'Connor *et al*., Phylogenetic support for a specialized clade of Cretaceous enantiornithine birds with information from a new species. *J. Vertebr. Paleontol.* **29**, 188–204 (2009).
11. D. J. Field *et al*., Complete *Ichthyornis* skull illuminates mosaic assembly of the avian head. *Nature* **557**, 96–100 (2018).
12. M. Wang, Z. Zhou, A new adult specimen of the basalmost ornithuromorph bird Archaeorhynchus spathula (Aves: Ornithuromorpha) and its implications for early avian ontogeny. *J. Syst. Palaeontology* **15**, 1–18 (2017).

13. S. Zhou, Z. Zhou, J. K. O'Connor, Anatomy of the basal ornithuromorph bird Archaeorhynchus spathula from the Early Cretaceous of Liaoning, China. *J. Vertebr. Paleontol.* **33**, 141–152 (2013).
14. Z. Zhou, F. Zhang, A beaked basal ornithurine bird (Aves, Ornithurae) from the Lower Cretaceous of China. *Zool. Scr.* **35**, 363–373 (2006).
15. G. De Beer, *The Development of the Vertebrate Skull* (Clarendon Press, 1937).
16. G. F. Couly, P. M. Coltey, N. M. Le Douarin, The triple origin of skull in higher vertebrates: A study in quail-chick chimeras. *Development* **117**, 409–429 (1993).
17. K. Kardong, *Vertebrates: Comparative Anatomy, Function, Evolution* (McGraw-Hill Higher Education, 2014).
18. M. K. Vickaryous, W. M. Olson, "Sesamoids and ossicles in the appendicular skeleton" in *Fins into Limbs: Evolution, Development and Transformation*, B. K. Hall, Ed. (University of Chicago Press, Chicago, 2007), pp. 323–341.
19. X. Zheng, J. K. O'Connor, X. Wang, Y. Wang, Z. Zhou, Reinterpretation of a previously described Jehol bird clarifies early trophic evolution in the Ornithuromorpha. *Proc. R. Soc. B* **285**, 20172494 (2018).
20. D. R. Carter, Mechanical loading history and skeletal biology. *J. Biomech.* **20**, 1095–1109 (1987).
21. P. D. F. Murray, D. B. Drachman, The role of movement in the development of joints and related structures: The head and neck in the chick embryo. *J. Embryol. Exp. Morphol.* **22**, 349–371 (1969).
22. B. K. Hall, Immobilization and cartilage transformation into bone in the embryonic chick. *Anat. Rec.* **173**, 391–403 (1972).
23. G. B. Müller, Embryonic motility: Environmental influences and evolutionary innovation. *Evol. Dev.* **5**, 56–60 (2003).
24. X. Zheng *et al*., New specimens of Yanornis indicate a piscivorous diet and modern alimentary canal. *PLoS One* **9**, e95036 (2014).
25. Z. Zhou, J. Clarke, F. Zhang, O. Wings, Gastroliths in Yanornis: An indication of the earliest radical diet-switching and gizzard plasticity in the lineage leading to living birds? *Naturwissenschaften* **91**, 571–574 (2004).
26. J. K. O'Connor, The trophic habits of early birds. *Palaeogeogr. Palaeoclimatol. Palaeoecol.* **513**, 178–195 (2019).
27. Z. Zhou, F. Zhang, Two new ornithurine birds from the Early Cretaceous of western Liaoning, China. *Chin. Sci. Bull.* **46**, 1258–1264 (2001).
28. S. Wang *et al*., Heterochronic truncation of odontogenesis in theropod dinosaurs provides insight into the macroevolution of avian beaks. *Proc. Natl. Acad. Sci. U.S.A.* **114**, 10930–10935 (2017).
29. M. R. Crole, J. T. Soley, Persistence of Meckel's cartilage in sub-adult Struthio camelus and Dromaius novaehollandiae. *Acta Zool.*, 10.1111/azo.12285 (2018).
30. H. I. Roach, J. Erenpreisa, T. Aigner, Osteogenic differentiation of hypertrophic chondrocytes involves asymmetric cell divisions and apoptosis. *J. Cell Biol.* **131**, 483–494 (1995).
31. C. Barreto, R. M. Albrecht, D. E. Bjorling, J. R. Horner, N. J. Wilsman, Evidence of the growth plate and the growth of long bones in juvenile dinosaurs. *Science* **262**, 2020–2023 (1993).
32. B. K. Hall, "Cartilage" in *Bones and Cartilage: Developmental and Evolutionary Skeletal Biology* (Academic Press, San Diego, 2005), pp. 33–47.
33. B. K. Hall, "The evolution of the neural crest in vertebrates" in *Regulatory Processes in Development: The Legacy of Sven Hörstadius Wenner-Gren International Series, Volume 76*, C.-O. Jacobson, L. Olsson, T. Laurent, Eds. (Portland Press, 2000), pp. 101–113.
34. B. K. Hall, The distribution and fate of the adventitious cartilage in the skull of the eastern rosella, *Platycerus eximius* (Aves: Psittaciformes). *Aust. J. Zool.* **15**, 685–698 (1967).
35. A. M. Bailleul, L. M. Witmer, C. M. Holliday, Cranial joint histology in the mallard duck (Anas platyrhynchos): New insights on avian cranial kinesis. *J. Anat.* **230**, 444–460 (2017).
36. D. Smith-Paredes *et al*., Dinosaur ossification centres in embryonic birds uncover developmental evolution of the skull. *Nat. Ecol. Evol.* **2**, 1966–1973 (2018).
37. T. F. Schilling, P. Le Pabic, "Neural crest cells in craniofacial skeletal development" in *Neural Crest Cell Differentiation and Disease*, P. Trainor, Ed. (Elsevier, 2014), pp. 127–151.
38. K. E. Campbell Jr, E. P. Tonni, Preliminary observations on the paleobiology and evolution of teratorns (Aves: Teratornithidae). *J. Vertebr. Paleontol.* **1**, 265–272 (1981).
39. M. Vickaryous, A. Russell, P. J. Currie, "Cranial ornamentation of ankylosaurs: Reappraisal of developmental hypotheses" in *The Armored Dinosaurs*, K. Carpenter, Ed. (Indiana University Press, Bloomington, 2001) pp. 318–340.
40. A. L. Romanoff, *The Avian Embryo. Structural and Functional Development* (MacMillan, New York, 1960).
41. T. L. Hieronymus, L. M. Witmer, Homology and evolution of avian compound rhamphothecae. *Auk* **127**, 590–604 (2010).
42. J. J. Baumel, L. M. Witmer, "Osteologia" in *Handbook of Avian Anatomy: Nomina Anatomica Avium*, J. J. Baumel, Ed. (Publications of the Nuttall Ornithological Club, 1993), pp. 45–132.
43. M. T. Jollie, The head skeleton of the chicken and remarks on the anatomy of this region in other birds. *J. Morphol.* **100**, 389–436 (1957).
44. M. Mina, B. Havens, D. A. Velonis, FGF signaling in mandibular skeletogenesis. *Orthod. Craniofac. Res.* **10**, 59–66 (2007). Corrected in: *Orthod. Craniofac. Res.* **10**, 235 (2007).
45. W. K. Parker, VIII. On the structure and development of the skull in the ostrich tribe. *Philos. Trans. R. Soc. Lond.* **156**, 113–183 (1866).
46. M. Webb, The ontogeny of the cranial bones, cranial peripheral and cranial parasympathetic nerves, together with a study of the visceral muscles of Struthio. *Acta Zool.* **38**, 81–203 (1957).
47. B. F. Eames, R. A. Schneider, The genesis of cartilage size and shape during development and evolution. *Development* **135**, 3947–3958 (2008).
48. E. J. Lessner, C. A. Gant, T. L. Hieronymus, M. K. Vickaryous, C. M. Holliday, Anatomy and ontogeny of the mandibular symphysis in Alligator mississippiensis. *Anat. Rec. (Hoboken)* **302**, 1696–1708 (2019).
49. B. K. Hall, "Tendons and Sesamoids" in *Bones and Cartilage* (Academic Press, San Diego, 2005), pp. 115–123.
50. S. Regnault, A. A. Pitsillides, J. R. Hutchinson, Structure, ontogeny and evolution of the patellar tendon in emus (Dromaius novaehollandiae) and other palaeognath birds. *PeerJ* **2**, e711 (2014).
51. G. A. Bohórquez Mahecha, C. Aparecida de Oliveira, An additional bone in the sclera of the eyes of owls and the common potoo (Nictibius griseus) and its role in the contraction of the nictitating membrane. *Acta Anat. (Basel)* **163**, 201–211 (1998).
52. P. Burton, Structure of the depressor mandibulae muscle in the Kokako Callaeas cinerea. *Ibis* **115**, 138–140 (1973).
53. S. Regnault, V. R. Allen, K. P. Chadwick, J. R. Hutchinson, Analysis of the moment arms and kinematics of ostrich (Struthio camelus) double patellar sesamoids. *J. Exp. Zool. A Ecol. Integr. Physiol.* **327**, 163–171 (2017).
54. M. K. Vickaryous, B. K. Hall, Development of the dermal skeleton in *Alligator mississippiensis* (Archosauria, Crocodylia) with comments on the homology of osteoderms. *J. Morphol.* **269**, 398–422 (2008).
55. W. J. Landis, F. H. Silver, The structure and function of normally mineralizing avian tendons. *Comp. Biochem. Physiol. A Mol. Integr. Physiol.* **133**, 1135–1157 (2002).
56. B. K. Hall, Descent with modification: The unity underlying homology and homoplasy as seen through an analysis of development and evolution. *Biol. Rev. Camb. Philos. Soc.* **78**, 409–433 (2003).
57. J. Y. Sire, P. C. Donoghue, M. K. Vickaryous, Origin and evolution of the integumentary skeleton in non-tetrapod vertebrates. *J. Anat.* **214**, 409–440 (2009).
58. B.-A. S. Bhullar *et al*., How to make a bird skull: Major transitions in the evolution of the avian cranium, paedomorphosis, and the beak as a surrogate hand. *Integr. Comp. Biol.* **56**, 389–403 (2016).
59. A. P. Summers, T. J. Koob, The evolution of tendon–Morphology and material properties. *Comp. Biochem. Physiol. A Mol. Integr. Physiol.* **133**, 1159–1170 (2002).
60. B. K. Hall, Selective proliferation and accumulation of chondroprogenitor cells as the mode of action of biomechanical factors during secondary chondrogenesis. *Teratology* **20**, 81–91 (1979).
61. B. K. Hall, The role of movement and tissue interactions in the development and growth of bone and secondary cartilage in the clavicle of the embryonic chick. *J. Embryol. Exp. Morphol.* **93**, 133–152 (1986).
62. R. C. Solem, B. F. Eames, M. Tokita, R. A. Schneider, Mesenchymal and mechanical mechanisms of secondary cartilage induction. *Dev. Biol.* **356**, 28–39 (2011).
63. E. R. Myers, V. C. Mow, "Biomechanics of cartilage and its response to biomechanical stimuli" in *Cartilage, Structure, Junction, and Biochemistry*, B. Hall, Ed. (Academic, 1983), pp. 313–337.
64. J. M. Mansour, "Biomechanics of cartilage" in *Kinesiology: The Mechanics and Pathomechanics of Human Movement*, C. A. Oatis, Ed. (Lippincott, Williams and Wilkins, 2003), pp. 66–79.
65. M. Persson, The role of movements in the development of sutural and diarthrodial joints tested by long-term paralysis of chick embryos. *J. Anat.* **137**, 591–599 (1983).
66. W. J. Bock, Kinetics of the avian skull. *J. Morphol.* **114**, 1–41 (1964).
67. R. G. Bout, G. A. Zweers, The role of cranial kinesis in birds. *Comp. Biochem. Physiol. A Mol. Integr. Physiol.* **131**, 197–205 (2001).
68. S. M. Estrella, J. A. Masero, The use of distal rhynchokinesis by birds feeding in water. *J. Exp. Biol.* **210**, 3757–3762 (2007).
69. A. M. Bailleul, J. O'Connor, M. H. Schweitzer, Dinosaur paleohistology: Review, trends and new avenues of investigation. *PeerJ* **7**, e7764 (2019).
70. A. M. Bailleul, C. M. Holliday, Joint histology in Alligator mississippiensis challenges the identification of synovial joints in fossil archosaurs and inferences of cranial kinesis. *Proc. R. Soc. B* **284**, 20170038 (2017).
71. A. M. Bailleul, B. K. Hall, J. R. Horner, First evidence of dinosaurian secondary cartilage in the post-hatching skull of *Hypacrosaurus stebingeri* (Dinosauria, Ornithischia). *PLoS One* **7**, e36112 (2012).
72. V. Hamburger, R. Oppenheim, Prehatching motility and hatching behavior in the chick. *J. Exp. Zool.* **166**, 171–203 (1967).
73. B. M. Freeman, M. A. Vince, Eds., *Development of the Avian Embryo: A Behavioural and Physiological Study* (Springer, 1974).
74. B. K. Hall, The fate of adventitious and embryonic articular cartilage in the skull of the common fowl, *Gallus domesticus* (Aves: Phasianidae). *Aust. J. Zool.* **16**, 795–805 (1968).
75. D. B. Drachman, L. Sokoloff, The role of movement in embryonic joint development. *Dev. Biol.* **14**, 401–420 (1966).
76. M. L. Habegger, "Functional morphology and feeding mechanics of billfishes." PhD thesis, University of South Florida, Tampa, FL (2014)
77. L. Habegger *et al*., Feeding biomechanics in billfishes: Investigating the role of the rostrum through finite element analysis. *Anat. Rec. (Hoboken)*, 10.1002/ar.24059 (2019).
78. C. M. Holliday, N. M. Gardner, S. M. Paesani, M. Douthitt, J. L. Ratliff, Microanatomy of the mandibular symphysis in lizards: Patterns in fiber orientation and Meckel's cartilage and their significance in cranial evolution. *Anat. Rec. (Hoboken)* **293**, 1350–1359 (2010).
79. M. Goret-Nicaise, A. Dhem, Presence of chondroid tissue in the symphyseal region of the growing human mandible. *Acta Anat. (Basel)* **113**, 189–195 (1982).

80. M. Goret-Nicaise, B. Lengele, A. Dhem, The function of Meckel's and secondary cartilages in the histomorphogenesis of the cat mandibular symphysis. *Arch. Anat. Microsc. Morphol. Exp.* **73**, 291–303 (1984).
81. A. M. Bailleul, C. Nyssen-Behets, B. Lengelé, B. K. Hall, J. R. Horner, Chondroid bone in dinosaur embryos and nestlings (Ornithischia: Hadrosauridae): Insights into the growth of the skull and the evolution of skeletal tissues. *C. R. Palevol* **15**, 49–64 (2016).
82. B. Berkovitz, P. Sloan, Attachment tissues of the teeth in Caiman sclerops (Crocodilia). *J. Zool.* **187**, 179–194 (1979).
83. S. J. Cunningham *et al*., The anatomy of the bill tip of kiwi and associated somatosensory regions of the brain: Comparisons with shorebirds. *PLoS One* **8**, e80036 (2013).
84. S. J. Cunningham *et al*., Bill morphology of ibises suggests a remote-tactile sensory system for prey detection. *Auk* **127**, 308–316 (2010).
85. A. R. Cuff, E. J. Rayfield, Retrodeformation and muscular reconstruction of ornithomimosaurian dinosaur crania. *PeerJ* **3**, e1093 (2015).
86. Y. Kobayashi, J. Lu, A new ornithomimid dinosaur with gregarious habits from the Late Cretaceous of China. *Acta Palaeontol. Pol.* **48**, 235–259 (2003).
87. A. Louchart, L. Viriot, From snout to beak: The loss of teeth in birds. *Trends Ecol. Evol.* **26**, 663–673 (2011).
88. V. K. Sarin, G. M. Erickson, N. J. Giori, A. G. Bergman, D. R. Carter, Coincident development of sesamoid bones and clues to their evolution. *Anat. Rec.* **257**, 174–180 (1999).
89. L. M. Chiappe, S.-A. Ji, Q. Ji, M. A. Norell, Anatomy and systematics of the Confuciusornithidae (Theropoda, Aves) from the late Mesozoic of northeastern China. *Bull. Am. Mus. Nat. Hist.*, **242**, 1–89 (1999).
90. H. Hu *et al*., Evolution of the vomer and its implications for cranial kinesis in Paraves. *Proc. Natl. Acad. Sci. U.S.A.* **116**, 19571–19578 (2019).
91. A. Bailleul, Z. Li, Yanornis. Open Science Framework, OSF. https://osf.io/q9xsp/. Deposited 30 October 2019.
92. H. F. Steedman, Alcian blue 8GS: A new stain for mucin. *Q. J. Microsc. Sci.* **91**, 477–479 (1950).
93. P. E. Witten, B. K. Hall, Seasonal changes in the lower jaw skeleton in male Atlantic salmon (Salmo salar L.): Remodelling and regression of the kype after spawning. *J. Anat.* **203**, 435–450 (2003).